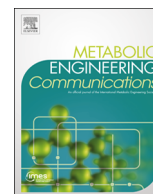Contents lists available at ScienceDirect

Metabolic Engineering Communications

journal homepage: www.elsevier.com/locate/mec

Improved sugar-free succinate production by *Synechocystis* sp. PCC 6803 following identification of the limiting steps in glycogen catabolism

Tomohisa Hasunuma [a,*], Mami Matsuda [a], Akihiko Kondo [b,c]

[a] *Organization of Advanced Science and Technology, Kobe University, 1-1 Rokkodai, Nada, Kobe 657-8501, Japan*
[b] *Biomass Engineering Program, RIKEN, 1-7-22 Suehiro, Tsurumi, Yokohama, Kanagawa 230-0045, Japan*
[c] *Department of Chemical Science and Engineering, Graduate School of Engineering, Kobe University, 1-1 Rokkodai, Nada, Kobe 657-8501, Japan*

ARTICLE INFO

ABSTRACT

Succinate produced by microorganisms can replace currently used petroleum-based succinate but typically requires mono- or poly-saccharides as a feedstock. The cyanobacterium *Synechocystis* sp. PCC6803 can produce organic acids such as succinate from CO_2 not supplemented with sugars under dark anoxic conditions using an unknown metabolic pathway. The TCA cycle in cyanobacteria branches into oxidative and reductive routes. Time-course analyses of the metabolome, transcriptome and metabolic turnover described here revealed dynamic changes in the metabolism of *Synechocystis* sp. PCC6803 cultivated under dark anoxic conditions, allowing identification of the carbon flow and rate-limiting steps in glycogen catabolism. Glycogen biosynthesized from CO_2 assimilated during periods of light exposure is catabolized to succinate via glycolysis, the anaplerotic pathway, and the reductive TCA cycle under dark anoxic conditions. Expression of the phospho*enol*pyruvate (PEP) carboxylase gene (*ppc*) was identified as a rate-limiting step in succinate biosynthesis and this rate limitation was alleviated by *ppc* overexpression, resulting in improved succinate excretion. The sugar-free succinate production was further enhanced by the addition of bicarbonate. *In vivo* labeling with $NaH^{13}CO_3$ clearly showed carbon incorporation into succinate via the anaplerotic pathway. Bicarbonate is in equilibrium with CO_2. Succinate production by *Synechocystis* sp. PCC6803 therefore holds significant promise for CO_2 capture and utilization.

1. Introduction

The issue of fossil resource depletion and global warming has prompted research on the sustainable production of environmentally benign fuels and chemicals. In particular, the utilization of biomass as a starting material for the production of fuels and chemicals has attracted considerable recent attention (Bozell and Peterson, 2010; Choi et al., 2015). The "biorefinery" is a manufacturing process for producing a wide variety of chemicals from biomass and is a promising alternative to conventional oil refinery processes. The use of bio-based chemicals can help reduce the amount of CO_2 emitted by fossil fuel combustion.

Photosynthetic algae are of increasing interest for the sustainable production of bio-based fuels and chemicals because the cultivation of algae does not directly compete with terrestrial agricultural resources such as productive land and fresh water (Dismukes et al., 2008; Wijffels et al., 2013). Several species of microalgae and cyanobacteria can store significant amounts of energy-rich compounds such as lipids and polysaccharides (starch and glycogen) that can be utilized for the production of distinct bio-fuels, including bio-diesel and bio-ethanol (Aikawa et al., 2013, 2014). In particular, cyanobacteria are attractive because they are responsible for a substantial proportion of biomass in the hydrosphere (Partensky et al., 1999), and their metabolic pathways are more readily amenable to genetic modifications designed to enhance photosynthetic activity than are those of eukaryotic algae (Hasunuma et al., 2014). The genome of the unicellular cyanobacterium *Synechocystis* sp. PCC6803 (hereafter *Synechocystis* 6803) was sequenced in 1996 (Kaneko et al., 1996) and *Synechocystis* 6803 is one of the most extensively investigated cyanobacteria. *Synechocystis* 6803 was recently shown to directly convert CO_2 into commodity chemicals such as acetone, 2,3-butanediol, 3-hydroxypropionic acid, isobutanol and *n*-butanol following the application of metabolic engineering strategies such as overexpression, gene deletion, and tuning of inherent and heterologous metabolic pathways (Anfelt et al., 2015; Savakis et al., 2013; Varman et al., 2013; Wang et al., 2016; Zhou et al., 2012).

---

* Corresponding author.
  E-mail address: hasunuma@port.kobe-u.ac.jp (T. Hasunuma).

Succinic acid (1,2-ethanedicarboxylic acid) is likely to become an important chemical intermediate for the production of biodegradable plastics, polybutylene succinate, polyester polyols and polyurethanes (Cukalovic and Stevens, 2008; Delhomme et al., 2009). As a platform chemical, succinic acid can be chemically converted to other valuable chemicals such as 1,4-butanediol, γ-butyrolactone, tetrahydrofuran and *N*-methylpyrrolidone, which can be used as surfactants and ion chelators, as well as being used in the food and pharmaceutical industries (Akhtar et al., 2014). The current market size for succinate is about 30,000–50,000 t per year, while the market potential is expected to be more than 700,000 t per year by 2020 (Choi et al., 2015). Succinate can be produced from renewable resources, including sugars and starchy/lignocellulosic biomass, by biotechnological approaches (Akhtar et al., 2014; Chen and Nielsen, 2013; Tsuge et al., 2013). Bio-based succinate has been generated using native producers such as rumen bacteria (e. g., *Actinobacillus succinogenes*, *Anaerobiospirillum succiniciproducens*, and *Bacillus fragilis*) and certain fungi (e. g., *Fusarium*, *Aspergillus* and *Penicillium* species), and metabolically engineered microorganisms such as *Escherichia coli*, *Corynebacterium glutamicum* and *Saccharomyces cerevisiae* (Beauprez et al., 2010; Chen and Nielsen, 2013; Lee et al., 2014). However, such heterotrophic microorganisms need sugars or biomass feedstocks as carbon sources for succinate fermentation, and thus the supply of fermentation substrates remains a bottleneck to realizing the economical and energy-saving production of bio-based chemicals.

Synechocystis 6803 can excrete succinate in the absence of sugars by autofermentation under dark anoxic conditions (Osanai et al., 2015). Glycogen, the primary storage polysaccharide in cyanobacteria (Ball and Morell, 2003), is biosynthesized from CO_2 under phototrophic conditions, which might be catabolized to form a range of fermentation products under dark anoxic conditions. In other words, succinate can be directly produced from CO_2 without the addition of any other feedstock. However, metabolic flow during sugar catabolism has never been directly observed, and little is known about the mechanism that regulates succinate biosynthesis in cyanobacteria under dark anoxic conditions.

Metabolomics is the comprehensive analysis of a wide range of intracellular metabolites and has identified metabolites that play important roles in specific biological processes (Camañes et al., 2015; Diamond et al., 2015; Link et al., 2013). Recently, dynamic metabolic profiling, which directly measures the turnover of metabolic intermediates in cyanobacteria, was developed by combining *in vivo* ^{13}C-labeling of metabolites, metabolomics, and mass distribution analysis using mass spectrometry (MS) (Hasunuma et al., 2013). Such profiling enables kinetic visualization of carbon metabolism in central metabolic pathways such as glycolysis and the pentose phosphate pathway under phototrophic conditions (Hasunuma et al., 2014).

The present study investigated the organic acids released into the fermentation medium during dark anoxic cultivation of *Synechocystis* 6803. Time-course analysis of *Synechocystis* metabolomics and dynamic metabolic profiling were performed during cultivation to isolate the rate-limiting steps of cyanobacterial succinate biosynthesis. Moreover, the limiting step was removed by overexpression of the rate-limiting step gene and by controlling the components in the medium to improve succinic acid production.

2. Materials and methods

2.1. Strains and culture conditions

A GT strain of *Synechocystis* sp. PCC6803 (Williams, 1988),

which was adapted to utilize glucose as a carbon source, was grown in BG11 liquid medium (Rippka et al., 1979). Cells were pre-cultivated for 4 days in 500-mL flasks containing 150 mL BG11 medium and 20 mM Hepes-KOH (pH 7.8) in an NC350-HC plant chamber (Nippon Medical and Chemical Instruments Co., Ltd., Osaka, Japan) under continuous irradiation with photo-synthetically-active 50 μmol m^{-2} s^{-1} white light photons and with 100-rpm agitation at 30 °C. The preculture was adjusted to an initial optical density at 750 nm (OD_{750}) of 0.1. Cultivation was performed in a closed double-deck flask: the first stage contained 50 mL of 2 M $NaHCO_3/Na_2CO_3$ buffer at the pH required to obtain a CO_2 concentration of 1% (v/v), and the second stage contained 70 mL modified-BG11 medium (BG11 medium containing 5 mM NH_4Cl or 5 mM $NaNO_3$ as a nitrogen source and 50 mM Hepes-KOH, pH 7.8) (Hasunuma et al., 2014). The pre-cultured cells were inoculated into fresh modified-BG11 medium at a biomass concentration of 0.1 g dry cell weight (DCW) L^{-1} (OD_{750} of 0.4) and cultivated for 3 days under continuous irradiation with 100–110 μmol m^{-2} s^{-1} white light photons with 100-rpm agitation at 30 °C. The light intensity was measured in the center of the medium using an LI-250A light meter equipped with an LI-190SA quantum sensor (LI-COR, Lincoln, NE). The cell density in the medium was determined as DCW because a linear correlation was observed between DCW and optical density measured at OD_{750} using a UV mini spectrophotometer (Shimadzu, Kyoto, Japan).

2.2. Construction of recombinant strains

The *rbcL* terminator and downstream regions of slr0168 were amplified from *Synechocystis* 6803 genomic DNA by PCR using the primer set 5′-CCTCTAGAGTCGACCTGCAGGTTACAGTTTTGGCAATTAC-3′/5′-GCCAGCCCCAACACCTGACGCGTTTCCCACTTAGATAAAAAATCC-3′ and 5′-TCTAAGTGGGGAAACGCGTCAGGTGTTGGGGCTGGC-3′/5′-TGATTACGCCAAGCTTCTAAGTCAGCGTAAATCTGACAATG-3′, respectively, and then integrated into the *Pst*I and *Hind*III sites of pBluescript II SK(+) (Agilent Technologies, Palo Alto, CA) using an In-Fusion HD Cloning Kit (Takara Bio, Shiga, Japan) to yield pBluescript-TrbcL-slr0168. A kanamycin-resistance cassette and *rbcL* promoter were amplified from pCRII-TOPO (Invitrogen, Carlsbad, CA) and *Synechocystis* 6803 genomic DNA by PCR using the primer set 5′-CGGGCCCCCCCTCGAGCCGGAATTGCCAGCTGGGGC-3′/5′-TGGACTTTCTAATTAGAGCGGCCGCTCAGAAGAACTCGTCAAGA-3′ and 5′-TCTTGACGAGTTCTTCTGAGCGGCCGCTCTAATTAGAAAGTCCA-3′/5′-CCGGGGATCCTCTAGACATATGGGTCAGTCCTCCAT-3′, respectively. The amplified fragments were integrated into the *Xho*I and *Xba*I sites of pBluescript-TrbcL-slr0168 using an In-Fusion HD Cloning Kit to yield pBluescript-Km^r-PrbcL-TrbcL-slr0168. The upstream region of slr0168 was amplified from *Synechocystis* 6803 genomic DNA by PCR using the primer set 5′-TATAGGGCGAATTGGGTACCATGACTATTCAATACACCCCCCTAG-3′/5′-TACCGTCGACCTCGAGCACCAGACCAAAGCCGGGAATTTC-3′ and then integrated into the *Kpn*I and *Xho*I sites of pBluescript-Km^r-PrbcL-TrbcL-slr0168 using an In-Fusion HD Cloning Kit to yield pBluescript-slr0168-Km^r-PrbcL-TrbcL-slr0168. The *Nde*I site (CAT-ATG) of pUC19 (Takara Bio) was replaced with CACATG by digesting *Aat*II and *Eco*RI and inserting the synthetic DNA. Following the digestion of pBluescript-slr0168-Km^r-PrbcL-TrbcL-slr0168 with *Kpn*I and *Hind*III, the fragment containing slr0168 was integrated into the *Kpn*I/*Hind*III site of the modified pUC19 vector to yield pSKrbcL-slr0168. The trc promoter was amplified from pTrcHis vector (Invitrogen) by PCR using the primer set 5′-TTCTTCTGAGCGGCCGCCGACTGCACGGTGCACCAAT-3′/5′-TCGACTCTAGACATATGGGTCTGTTTCCTGTGTGAA-3′ and then integrated into the *Not*I and *Nde*I site of pSKrbcL-slr0168 to yield pSKtrc-slr0168. The *ppc* (sll0920) gene encoding phospho*enol*pyruvate (PEP) carboxylase was amplified from *Synechocystis* 6803 genomic

DNA by PCR using the primer set 5′-AGGAAACAGACCCA-TATGAACTTGGCAGTTCCTGC-3′/5′-AACCTGCAGGTCGACTCAAC-CAGTATTACGCA-3′. The resulting fragment was integrated into NdeI/SalI digested pSKtrc-slr0168 using an In-Fusion HD Cloning Kit to yield pSKtrc-slr0168/sll0920. The GT strain was transformed with pSKtrc-slr0168/sll0920 using a previously described method (Osanai et al., 2011) to yield strain Ppc-ox. Also, the plasmid pSKtrc-slr0168 was introduced into the GT strain to yield the vector control strain. Colonies resistant to 50 μg mL^{-1} kanamycin were selected, and isolation of a single colony was repeated to achieve complete segregation. The chromosomal integration of ppc and the plasmid-derived sequence was confirmed by PCR using the specific primers 5′-ATGGCACCGATGCGGAATCCCAACA-GATTGCCTTTGAC-3′ and 5′-CACGTTGGGTCCCAAGTTTGTGCTGTGG CTGATGCCAT-3′.

2.3. Batch fermentation under anaerobic conditions

After cultivation under phototrophic conditions for 3 days, the cells were collected by filtration using 1-μm pore size polytetra-fluoroethylene (PTFE) filter disks (Omnipore; Millipore, Billerica, MA) and transferred into 50 mM Hepes-KOH (pH 7.8). All fermentations were performed at 30 °C under anaerobic conditions with an agitation speed of 170 rpm in 30 mL closed bottles containing 10 mL cell suspension. The initial cell concentration was adjusted to 5 g DCW L^{-1} (OD$_{750}$ of 20). The effects of adding NaHCO$_3$ on dark anoxic cultivation of Synechocystis 6803 were investigated using 100 mM Hepes-KOH (pH 7.8) to stabilize the pH of the medium. The concentrations of organic acids in the fermentation medium were analyzed using a high performance liquid chromatography (HPLC) system (Shimadzu) equipped with an Aminex HPX-87H column (300 mm × 7.8 mm; Bio-Rad, Hercules, CA) and an RID-10A refractive index detector (Shimadzu). The HPLC system was operated at 50 °C using 5 mM H$_2$SO$_4$ as the mobile phase at a flow rate of 0.6 mL min^{-1}.

2.4. Analysis of intracellular metabolites

Samples for intracellular metabolite analysis were prepared as described previously (Hasunuma et al., 2014). Cyanobacterial cells equivalent to 5 mg DCW were collected from fermentation vessels and immediately filtered using 1-μm pore size PTFE filter disks (Omnipore). After washing the filter disks with 20 mM ammonium carbonate pre-chilled to 4 °C, cells retained on the filters were immediately placed into 2 mL pre-cooled (−30 °C) methanol containing 37.38 μM ʟ-methionine sulfone and 37.38 μM piper-azine-1,4-bis(2-ethanesulfonic acid) as internal standards for mass analysis. Cells were suspended by vortexing, then 0.5 mL of the cell suspension was mixed with 0.2 mL of pre-cooled (4 °C) water and 0.5 mL of chloroform at 4 °C. After vortexing for 30 s, the aqueous and organic layers were separated by centrifugation at 14,000xg for 5 min at 4 °C. The aqueous layer (500 μL) was filtered through a Millipore 5 kDa cut-off membrane to remove solubilized proteins. Water was evaporated from the aqueous-layer extracts under vacuum using a FreeZone 2.5 Plus freeze dryer system (Labconco, Kansas City, MO) and the dried metabolites were dissolved in 20 μL of Milli-Q water. The metabolites were analyzed using a capillary electrophoresis-mass spectrometry (CE-MS) system (CE, Agilent G7100; MS, Agilent G6224AA LC/MSD TOF; Agilent Technologies) controlled by MassHunter Workstation Data Acquisition software (Agilent Technologies), as described previously (Hasunuma et al., 2013).

2.5. Global gene expression analysis

Total RNA was obtained after 3, 6, 24, and 48 h of fermentation

using a Total RNA Isolation Mini Kit (Agilent Technologies) according to the manufacturer's protocol. RNA concentration and quality were measured using a NanoDrop ND-1000 spectro-photometer (NanoDrop, Wilmington, DE) and an Agilent 2100 Bioanalyzer (Agilent Technologies), respectively. cDNA was re-verse-transcribed and labeled with cyanine 3-CTP using a Low-Input Quick Amp Labeling Kit (Agilent Technologies) for hy-bridization in 8 × 15k microarrays designed by the author. Hy-bridization was performed at 65 °C for 17 h and the arrays were scanned using an Agilent Single-Color DNA Microarray Scanner (Agilent Technologies). Gene expression levels were normalized per chip. GeneSpring GX ver. 11.5.1 software (Agilent Technologies) was used to analyze the fold-change in expression data. Each biological sample subjected to microarray analysis was analyzed in triplicate.

2.6. Analysis of intracellular glycogen

Synechocystis cells were harvested from fermentation vessels using PTFE filter disks, as described above. Cells on the filters were washed with 20 mM ammonium carbonate, then immediately frozen in liquid nitrogen and freeze-dried using a freeze dryer (Labconco). Glycogen was extracted as described previously (Izumi et al., 2013). Briefly, glycogen was extracted from 5 mg dry weight cells with 100 μL aqueous KOH (30%, w/v) by incubation in a 90 °C heat block for 90 min, followed by placement on ice. Ethanol (300 μL) pre-chilled to 4 °C was added to the cooled extracts and the extracts were incubated on ice for 1 h. After centrifugation at 7500xg for 5 min at 4 °C, the resulting pellet was washed three times with cold ethanol, then dried for 30 min at 80 °C. Recon-stitution in 100 μL water and centrifugation at 14,000xg for 5 min provided the glycogen extract as the supernatant. The glycogen concentration was determined by measuring the glucose released from glycogen by enzymatic hydrolysis. Glycogen extract (50 μL) was mixed with 40 μL of 800 mM sodium acetate buffer (adjusted to pH 4.9 with acetate) and 10 μL of 400 U mL^{-1} glucoamylase (TOYOBO, Shiga, Japan), then incubated with 200 rpm agitation at 50 °C for 2 h. The enzyme was then denatured at 95 °C for 20 min and the mixture was centrifuged at 14,000xg for 5 min at 4 °C. The supernatant was applied to an HPLC system to determine the amount of glucose hydrolyzed from glycogen. The HPLC system was equipped with an Aminex HPX-87 h column and an RID-10A refractive index detector, as described above.

2.7. Enzyme assay

Glycogen phosphorylase (GP) activity was measured according to a previous method (Andersen and Westergaard, 2002) with minor modifications. Synechocystis cells were cultivated for 72 h under phototrophic conditions followed by 24 h dark anoxic cul-tivation. The culture (100 μL) was centrifuged at 6000xg for 10 min at 4 °C and the supernatant was discarded. The cells were washed with extraction buffer (18 mM KH$_2$PO$_4$, 27 mM Na$_2$HPO$_4$, 15 mM MgCl$_2$, and 100 μM EDTA, pH 8.0) and suspended in 3 mL of extraction buffer, then disrupted by sonication. Unbroken cells and cell debris were removed by centrifugation (20,000xg for 20 min at 4 °C) and the supernatant was used as a protein extract for the enzyme assay. A 1.5 mL aliquot of reaction mixture con-tained 100 μL of the protein extract and 1.4 mL of a solution comprising 18 mM KH$_2$PO$_4$, 27 mM Na$_2$HPO$_4$, 15 mM MgCl$_2$, 100 μM EDTA, 340 μM NADP$^+$, 4 μM glucose 1, 6-bisphosphate, 6 units mL^{-1} glucose 6-phosphate dehydrogenase, 0.8 units mL^{-1} phosphoglucomutase and 2 mg mL^{-1} glycogen (from oyster, Na-calai Tesque, Inc., Kyoto, Japan). The same mixture but without the glycogen was used as a control. Enzyme activities were de-termined by measuring the production of NADPH in the reaction

mixtures as a change in absorbance at 340 nm. PEP carboxylase activity was measured according to a previous method (Chen et al., 2002). *Synechocystis* cells were cultivated for 24 h under phototrophic conditions. A 1.5 mL aliquot of reaction mixture contained 50 μL of the protein extract and 1.45 mL of a solution comprising 50 mM Tris–HCl (pH 7.5), 15 mM MgSO$_4$, 10 mM KHCO$_3$, 100 μM NADH, 1 unit mL^{-1} malate dehydrogenase, and 5 mM PEP. The same mixture but without the PEP was used as a control. Enzyme activities were determined by measuring the oxidation of NADH in the reaction mixtures as a change in absorbance at 340 nm. The reactions were performed directly in cuvettes. Protein concentrations were determined with the BCA method as described previously (Hasunuma et al., 2013). The data are presented as averages of three independent assays.

2.8. ^{13}C-labeling experiment

In-vivo ^{13}C-labeling was performed to analyze the turnover of metabolites in cyanobacteria. Anaerobic fermentation was initiated by suspending cells in 50 mM Hepes-KOH (pH 7.8) containing 2 g L^{-1} [U-^{13}C] glucose or 100 mM ^{13}C-bicarbonate. After labeling for 0–6 h, the cells were collected by filtration and processed as described for metabolite analysis. Extracted metabolites were analyzed using CE-MS. Mass spectral peaks of biological origin were identified manually by searching for mass shifts between the ^{12}C- and ^{13}C-mass spectra. The ^{13}C fraction of the metabolites was calculated as described previously (Hasunuma et al., 2010). The relative isotopomer abundance (m_i) for each metabolite incorporating i^{13}C atoms was calculated as follows:

$$m_i(\%) = \frac{M_i}{\sum_{j=0}^{n} M_j} \times 100$$

where M_i represents the isotopomer abundance for each metabolite incorporating i^{13}C atoms. The ^{13}C fraction of metabolites possessing n carbon atoms is calculated as follows:

$$^{13}\text{Cfraction}(\%) = \sum_{i=1}^{n} \frac{i \times m_i}{n}$$

3. Results

3.1. Organic acid production during autofermentation by Synechocystis cells

Synechocystis sp. PCC6803 cells were cultivated phototrophically in modified BG11 medium containing 5 mM NaNO$_3$ or NH$_4$Cl as the sole nitrogen source for 3 days, then the cells were transferred to 50 mM Hepes-KOH buffer (pH 7.8) to initiate fermentation under anaerobic conditions. NaNO$_3$ is the typical nitrogen source used in the cultivation of *Synechocystis* but a recent study (Osanai et al., 2015) used NH$_4$Cl instead; therefore, the two nitrogen sources were compared in this study. During the phototrophic cultivation, no succinate was detected in the medium.

As shown in Fig. 1, under dark anoxic conditions, significant concentrations of the organic acids acetate, 2-ketoglutarate, lactate, malate and succinate were secreted into the fermentation medium, irrespective of the nitrogen source used. The concentration of acetate in the fermentation medium increased with time, to more than 400 mg L^{-1} after 96 h fermentation, whereas the concentration of lactate plateaued at app. 60 mg L^{-1} after 24 h. Succinate production was initiated after 6 h of fermentation and increased with time to 100 mg L^{-1} after 96 h when NH$_4$Cl was used as the nitrogen source. After 72 h fermentation, fumarate concentration was 5 mg L^{-1} (data not shown). The concentrations of citrate, *iso*-citrate, fumarate and oxaloacetate in the fermentation
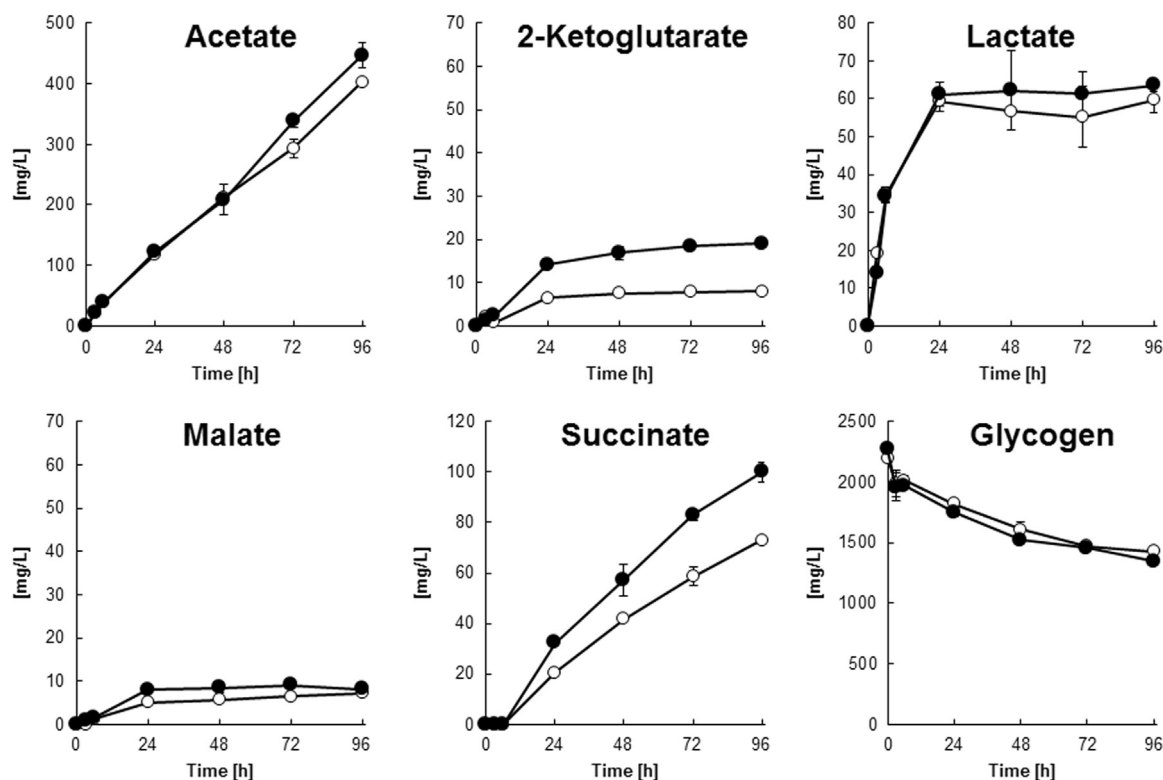

Fig. 1. Time-course of the production of organic acids secreted into the medium and glycogen utilization during dark anoxic fermentation by *Synechocystis* 6803 phototrophically cultivated in the presence of 5 mM NaNO$_3$ (open symbols) or 5 mM NH$_4$Cl (closed symbols) as the sole nitrogen source. Each data point represents the average ($\pm$ SD) of three independent experiments
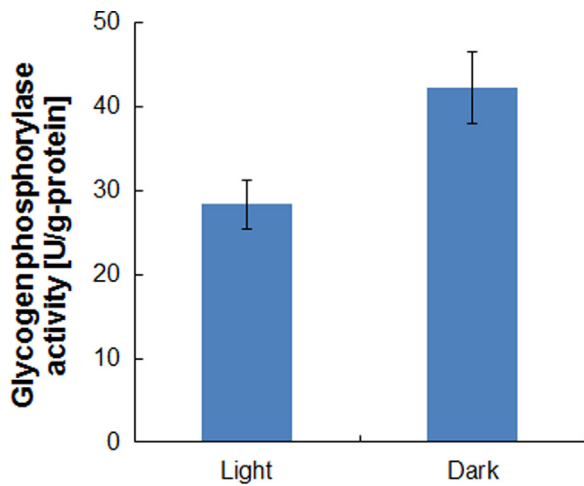
Fig. 2. Glycogen phosphorylase activity under light and dark anoxic conditions. The activity was measured after 72 h phototrophic cultivation and 24 h dark anoxic cultivation. Each data point represents the average ($\pm$SD) of three independent experiments.

medium were lower than $1\,mg\,L^{-1}$ (data not shown). NH_4Cl supported higher organic-acid production than did $NaNO_3$. The intracellular glycogen content decreased from 0.44 g-glycogen $g\text{-}DCW^{-1}$ when the cells were grown in medium containing $NaNO_3$ to 0.37 g-glycogen $g\text{-}DCW^{-1}$ when the cells were cultivated in the presence of NH_4Cl. Since the DCW decreased from $5.2\,g\,L^{-1}$ to $3.7\,g\,L^{-1}$ during 96-h fermentation, the glycogen in the fermentation vessel decreased from $2.3\,g\,L^{-1}$ to $1.3\,g\,L^{-1}$ (Fig. 1). The activity of glycogen phosphorylase (GP), which is involved in glycogen hydrolysis by cyanobacteria, was increased 1.5-fold by changing from light to dark anoxic cultivation conditions (Fig. 2).

3.2. Time-course transcriptome analysis during autofermentation

Time-course transcriptome analysis of *Synechocystis* cells grown in the presence of 5 mM NH_4Cl under anaerobic conditions was conducted using DNA microarrays. Switching to dark anoxic conditions resulted in a more than 2-fold increase in the expression level of 10 genes (Table 1) and a more than 2-fold decrease in the expression level of 43 genes (Table 2). The examination of genes involved in glycolysis and the tricarboxylic acid (TCA) cycle showed that the expression of *nifJ* (sll0741), which encodes

Table 1
Genes up-regulated under dark anoxic conditions[a].

ID	Gene	Fold change[b]			Description
		3 h	6 h	24 h	
slr1291	*ndhD2*	7.53	6.71	7.41	NAD(P)H-quinone oxidoreductase subunit 4
slr0518	*abfB*	5.67	5.24	6.10	arabinofuranosidase
sll0741	*nifJ*	2.53	1.32	1.27	pyruvate oxidoreductase
sll1894	*ribA*	2.39	1.72	1.34	riboflavin biosynthesis protein RibA
sll0248	*isiB*	2.16	2.08	2.48	flavodoxin FldA
sll0070	*purU*	1.67	1.73	2.53	formyltetrahydrofolate deformylase
slr0905	*bchE*	1.21	1.13	2.20	Mg-protoporphyrin IX monomethyl ester oxidative cyclase 66 kD subunit
sll1688	*thrC*	1.16	1.67	2.65	threonine synthase
slr1165	*sat*	1.13	1.14	2.43	sulfate adenylyltransferase
sll0938	*sll0938*	1.01	−1.06	2.38	aspartate transaminase

[a] Genes annotated in cyanobase (http://genome.microbedb. jp/cyanobase/Synechocystis) were selected.
[b] Fold change is the ratio of expression at 0 h to 3, 6 and 24 h. According to t-test, values were significantly different ($P < 0.05$).

pyruvate:ferredoxin oxidoreductase (PFO), was 2.53-fold upregulated after 3 h of cultivation under dark anoxic conditions (Table 1), and genes involved in redox reactions and in hydrogen production, such as *ndhD2* (slr1291) and *isiB* (sll0248), were also upregulated under these conditions. On the other hand, the following genes were all downregulated: *cbbA* (sll0018), which encodes fructose 1,6-bisphosphate (FBP) aldolase; *gap1* (slr0884), which encodes glyceraldehyde 3-phosphate (GAP) dehydrogenase involved in glycolysis; *rbcS* (slr0012) and *rbcX* (slr0011), involved in the activity of ribulose 1,5-bisphosphate carboxylase/oxygenase (Rubisco); *acnB* (slr0665), involved in the TCA cycle; *ppc* (sll0920), involved in anaplerosis; and *glnN* (slr0288), *glnA* (slr1756), gad (sll1641), *gltB* (sll1502), *argG* (slr0585) and *cysK* (slr1842), involved in amino acid metabolism (Table 2). Genes involved in light harvesting and in the photosystem, such as *psbC* (sll0851), *psbB* (slr0906), *psaJ* (sml0008), *psaF* (sll0819), *psbD2* (slr0927), *psaE* (ssr2831), *psaA* (slr1834) and *apcA* (slr2067), *psaL* (slr1655), *ctaB* (sll1899), *psaB* (slr1835), *psaC* (ssl0563), *psbU* (sll1194), *apcC* (ssr3383), *petD* (slr0343), showed decreased expression.

3.3. Time-course metabolome analysis during anaerobic cultivation

The intracellular metabolome in *Synechocystis* was measured at 0, 3, 6, 24, 48, 72 and 96 h after the initiation of anaerobic cultivation (Fig. 3). Thirty four hydrophilic metabolites, including amino acids, cofactors, organic acids, sugar nucleotides and sugar phosphates, were analyzed by CE-MS to investigate the metabolic profile of the cells during anaerobic cultivation.

The concentrations of many metabolites, such as ADP-glucose, glucose 6-phosphate (G6P), ribulose 1,5-bisphosphate (RuBP), ribulose 5-phosphate (Ru5P), 3-phosphoglycerate (3PGA), 2-phosphoglycerate (2PGA), PEP, acetyl-CoA, citrate, *cis*-aconitate, *iso*-citrate and alanine, transiently increased until 6 h of anaerobic cultivation, and then decreased. In contrast, intracellular malate, fumarate and succinate increased until 24 h, then gradually decreased until 72 h and then stabilized.

Glucose 1-phosphate (G1P), sedoheptulose 7-phosphate (S7P) and aspartate increased in concentration with time. FBP was present at significantly higher concentration than its breakdown products, dihydroxyacetone phosphate (DHAP) and GAP. The concentration of ATP increased up to 24 h of anaerobic cultivation, then decreased with time. Cells grown in the presence of NH_4Cl had a higher content of organic acids than cells grown in $NaNO_3$, although the concentrations of glycolysis-related metabolites were the same.

3.4. Metabolite turnover analysis under anaerobic conditions

No carbon source was supplied to cells growing under dark anoxic conditions, so glycogen was apparently converted to organic acids via glycolysis. However, to date there has been no report of the direct observation of glycogen and glucose catabolism.

During metabolism under steady state conditions, metabolites are replaced with newly synthesized compounds at a constant rate and the total amount of each metabolite remains unchanged. Therefore, the determination of time-course changes in the metabolome is insufficient to account for intracellular carbon flow. However, since the *Synechocystis* GT strain used in this study can utilize glucose as a carbon source, ^{13}C-glucose was added to the medium as a carbon source for the anaerobic cultivation of *Synechocystis,* and carbon flow during dark anaerobic cultivation was observed by tracer experiments.

^{13}C was incorporated into metabolites in *Synechocystis* cells following initiation of dark anoxic cultivation (Fig. 4). The ^{13}C fraction, defined as the ratio of ^{13}C to the total carbon in each metabolite, was calculated from the mass isotopomer

Table 2
Genes down-regulated under dark anoxic conditions[a].

ID	Gene	Fold change[b]			Description
		3 h	6 h	24 h	
sll0851	*psbC*	− 8.66	− 11.93	− 13.62	photosystem II CP43 protein
slr0906	*psbB*	− 6.06	− 6.88	− 12.70	photosystem II CP47 protein
sml0008	*psaJ*	− 6.05	− 7.10	− 5.85	photosystem I reaction center subunit IX
slr1643	*petH*	− 5.83	− 7.03	− 8.46	ferredoxin-NADP oxidoreductase
slr0012	*rbcS*	− 5.71	− 7.59	− 6.85	ribulose bisphosphate carboxylase small subunit
sll0819	*psaF*	− 5.62	− 6.72	− 4.78	photosystem I subunit III
sll1566	*ggpS*	− 4.57	− 5.09	− 3.32	glucosylglycerolphosphate synthase
sll0018	*cbbA*	− 4.47	− 4.43	− 6.46	fructose 1,6-bisphosphate aldolase
sll1535	*rfbP*	− 4.25	− 3.62	− 2.93	galactosyl-1-phosphate transferase
sll1577	*cpcB*	− 3.93	− 4.00	− 7.66	phycocyanin β subunit
sll1085	*glpD*	− 3.84	− 4.03	− 3.18	glycerol 3-phosphate dehydrogenase
slr0288	*glnN*	− 3.79	− 4.11	− 3.75	glutamate-ammonia ligase
slr0927	*psbD2*	− 3.58	− 4.24	− 5.83	photosystem II D2 protein
ssr2831	*psaE*	− 3.51	− 3.60	− 4.51	photosystem I reaction center subunit IV
slr0054	*dgkA*	− 3.30	− 4.01	− 5.11	diacylglycerol kinase
slr1756	*glnA*	− 3.10	− 3.16	− 3.18	glutamate-ammonia ligase
slr1834	*psaA*	− 3.04	− 5.36	− 9.34	photosystem I P700 chlorophyll a apoprotein A1
slr2067	*apcA*	− 2.99	− 3.07	− 5.93	allophycocyanin α chain
slr1655	*psaL*	− 2.85	− 2.57	− 3.20	photosystem I reaction center protein subunit XI
sll1899	*ctaB*	− 2.83	− 2.78	− 2.04	protoheme IX farnesyltransferase
slr0884	*gap1*	− 2.81	− 3.16	− 2.89	glyceraldehyde 3-phosphate dehydrogenase
slr1835	*psaB*	− 2.73	− 4.92	− 3.25	photosystem I P700 chlorophyll a apoprotein A2
sll1641	*gad*	− 2.71	− 2.46	− 2.93	glutamate decarboxylase
ssl0563	*psaC*	− 2.64	− 2.85	− 2.89	photosystem I subunit VII
sll1194	*psbU*	− 2.61	− 2.78	− 3.88	photosystem II complex extrinsic protein precursor U
sll1184	*ho1*	− 2.52	− 2.28	− 2.18	heme oxygenase
slr0261	*ndhH*	− 2.48	− 2.52	− 2.28	NAD(P)H-quinone oxidoreductase subunit H
sll0080	*argC*	− 2.47	− 2.48	− 2.61	N-acetyl-gamma-glutamyl-phosphate reductase
slr1022	*argD*	− 2.45	− 2.78	− 3.44	acetylornithine aminotransferase
ssr3383	*apcC*	− 2.44	− 2.45	− 1.66	phycobilisome LC linker polypeptide
sll0920	*ppc*	− 2.38	− 2.87	− 2.47	phosphoenolpyruvate carboxylase
slr0665	*acnB*	− 2.33	− 2.77	− 2.16	bifunctional aconitate hydratase 2/2-methylisocitrate dehydratase
slr0011	*rbcX*	− 2.28	− 2.62	− 3.95	possible RubisCO chaperonin
sll1502	*gltB*	− 2.08	− 2.41	− 2.69	ferredoxin-dependent glutamate synthase
slr0343	*petD*	− 1.85	− 1.83	− 2.77	cytochrome B6-f complex subunit IV
slr0585	*argG*	− 1.78	− 1.93	− 2.64	argininosuccinate synthase
sll0166	*hemD*	− 1.76	− 2.23	− 1.26	uroporphyrin-III synthase
sll1893	*hisF*	− 1.74	− 2.15	1.30	imidazole glycerol phosphate synthase subunit HisF
slr1830	*phbC*	− 1.49	− 1.75	− 1.45	poly(3-hydroxyalkanoate) synthase
slr1842	*cysK*	− 1.35	− 1.12	− 1.44	cysteine synthase
slr1239	*pntA*	− 1.29	− 1.81	− 4.34	NAD(P) transhydrogenase subunit alpha
slr1072	*yefA*	− 1.19	− 1.08	− 2.43	GDP-D-mannose dehydratase
sll0550	*flv3*	1.04	− 1.08	− 2.05	flavoprotein
slr1064	*rfbU*	1.16	1.14	− 2.86	mannosyltransferase B

[a] Genes annotated in cyanobase (http://genome.microbedb. jp/cyanobase/Synechocystis) were selected.
[b] Fold change is the ratio of expression at 0 h to 3, 6 and 24 h. According to *t*-test, values were significantly different ($P < 0.05$).

distributions. Glucose is phosphorylated to G6P by hexokinase, then metabolized through glycolysis and the pentose phosphate pathway. The ^{13}C fraction of glycolysis metabolites (G6P, F6P, FBP, 3PGA and PEP) and acetyl-CoA reached a maximum of more than 80% after 30 min of labeling, whereas organic acids showed slower ^{13}C incorporation. In particular, 2-ketoglutarate showed the lowest ^{13}C fraction among the metabolites involved in the cyanobacterial TCA cycle, suggesting that succinate is mainly formed from fumarate via the reductive TCA cycle. Lactate and amino acids such as alanine, glutamate and glutamine were labeled by ^{13}C, although their ^{13}C fractions were lower than that of their common precursor, PEP. These data clearly indicated that glucose is catabolized to organic acids and amino acids under anaerobic conditions. Note that the ^{13}C fraction of pyruvate could not be evaluated because of its low abundance in cells.

As shown in Fig. S1, glucose added to the medium was consumed after 24 h and glycogen consumption was repressed during glucose consumption. The amount of succinate produced during the first 48 h was increased from 57 mg L^{-1} to 74 mg L^{-1} by the addition of 2 g L^{-1} glucose.

3.5. Improvement of succinate production based on multiple-omic analyses

The results of dynamic metabolic profiling, shown in Fig. 4, revealed that the ^{13}C fraction of citrate, malate, fumarate and succinate increased more slowly than that of PEP and acetyl-CoA, suggesting that the generation of organic acids involved in the TCA cycle is a rate-limiting step for succinate production. As previously described (Hasunuma et al., 2010), the initial slope of the ^{13}C-fraction *versus* time curve indicates the turnover rate of the metabolite. Intracellular oxaloacetate could not be detected because of its low abundance, but malate showed a lower turnover rate than citrate (Fig. 4), suggesting that the anaplerotic pathway from PEP to oxaloacetate limits succinate production.

PEP carboxylase converts PEP to oxaloacetate and is encoded by *ppc* (sll0920). The expression of *ppc* in *Synechocystis* 6803 was enhanced by linking *ppc* to the trc promoter, then integrating into the slr0168 loci through homologous recombination. The chromosomal integration of *ppc* was confirmed by genomic PCR (Fig. S2). Ppc-ox demonstrated 3-fold higher PEP carboxylase activity
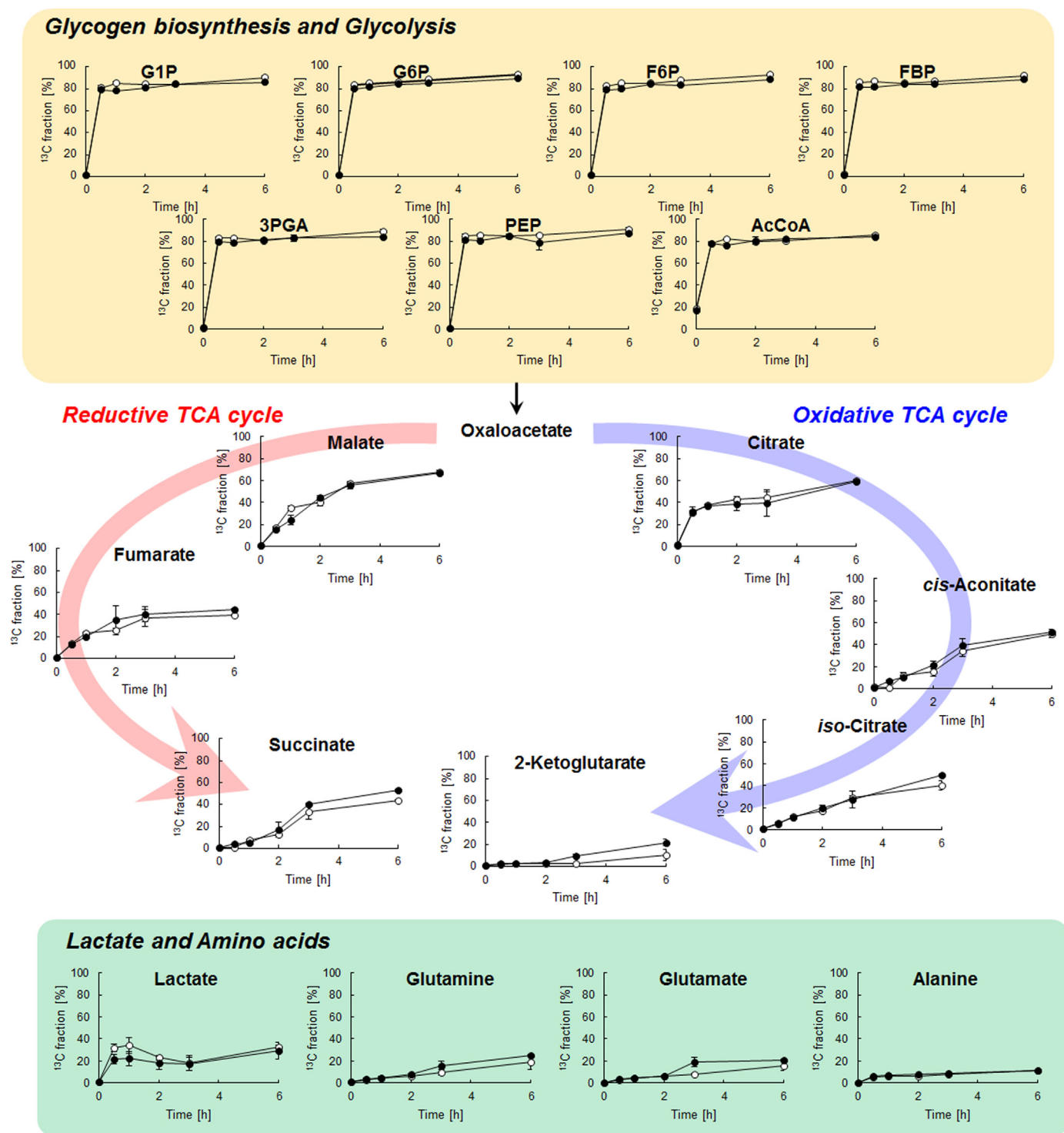
Fig. 3. Time-course changes of intracellular metabolite pool sizes during dark anoxic fermentation by *Synechocystis* 6803 phototrophically cultivated in the presence of 5 mM NaNO$_3$ (open symbols) or 5 mM NH$_4$Cl (closed symbols) as the sole nitrogen source. Two-fold upregulated and downregulated genes are shown in red and blue characters, respectively. A reaction catalyzed by ACL is shown with dashed lines. Abbreviations: FBP, fructose 1,6-bisphosphate; F6P, fructose 6-phosphate; GABA, γ-aminobutyrate; GAP, glyceraldehyde 3-phosphate; G1P, glucose 1-phosphate; G6P, glucose 6-phosphate; PEP, phospho*enol*pyruvate; 2PGA, 2-phosphoglycerate; 3PGA, 3-phosphoglycerate; R5P, ribose 5-phosphate; Ru5P, ribulose 5-phosphate; RuBP, ribulose 1,5-bisphosphate; S7P, sedoheptulose 7-phosphate; SBP, sedoheptulose 1,7-bisphosphate; DCW, dry cell weight. (For interpretation of the references to color in this figure legend, the reader is referred to the web version of this article.)

Fig. 4. Time-course changes in the metabolite ^{13}C fraction following the addition of ^{13}C-glucose to cultures of *Synechocystis* sp. PCC6803 phototrophically cultivated in the presence of 5 mM NaNO$_3$ (open symbols) or 5 mM NH$_4$Cl (closed symbols) as the sole nitrogen source. Each data point represents the average ($\pm$ SD) of three independent experiments.

than its vector control strain (VC) (Fig. S2). After 72 h fermentation, the recombinant *Synechocystis* strain, Ppc-ox, exhibited significantly higher production of succinate (140 mg L^{-1}) than VC (111 mg L^{-1}) (Fig. 5). Acetate production was also enhanced by overexpression of sll0920, whereas Ppc-ox showed lower lactate production than VC. Biomass monitored via OD$_{750}$ was similar between Ppc-ox and VC.

NaHCO$_3$ was added to the medium at the start of anaerobic cultivation of GT strain in order to further improve succinate

production. As shown in Fig. 6, succinate production increased as the concentration of NaHCO$_3$ increased and reached 185 mg L^{-1} after 72 h fermentation in the presence of 300 mM NaHCO$_3$. Lactate and acetate were as high as 1132 mg L^{-1} and 393 mg L^{-1}, respectively, in the presence of 500 mM NaHCO$_3$, and NaHCO$_3$ addition significantly increased the production of other organic acids such as citrate, fumarate, 2-ketoglutarate and malate that were below 6 mg L^{-1} in the absence of NaHCO$_3$. Furthermore, in the presence of 100 mM NaHCO$_3$, succinate production was
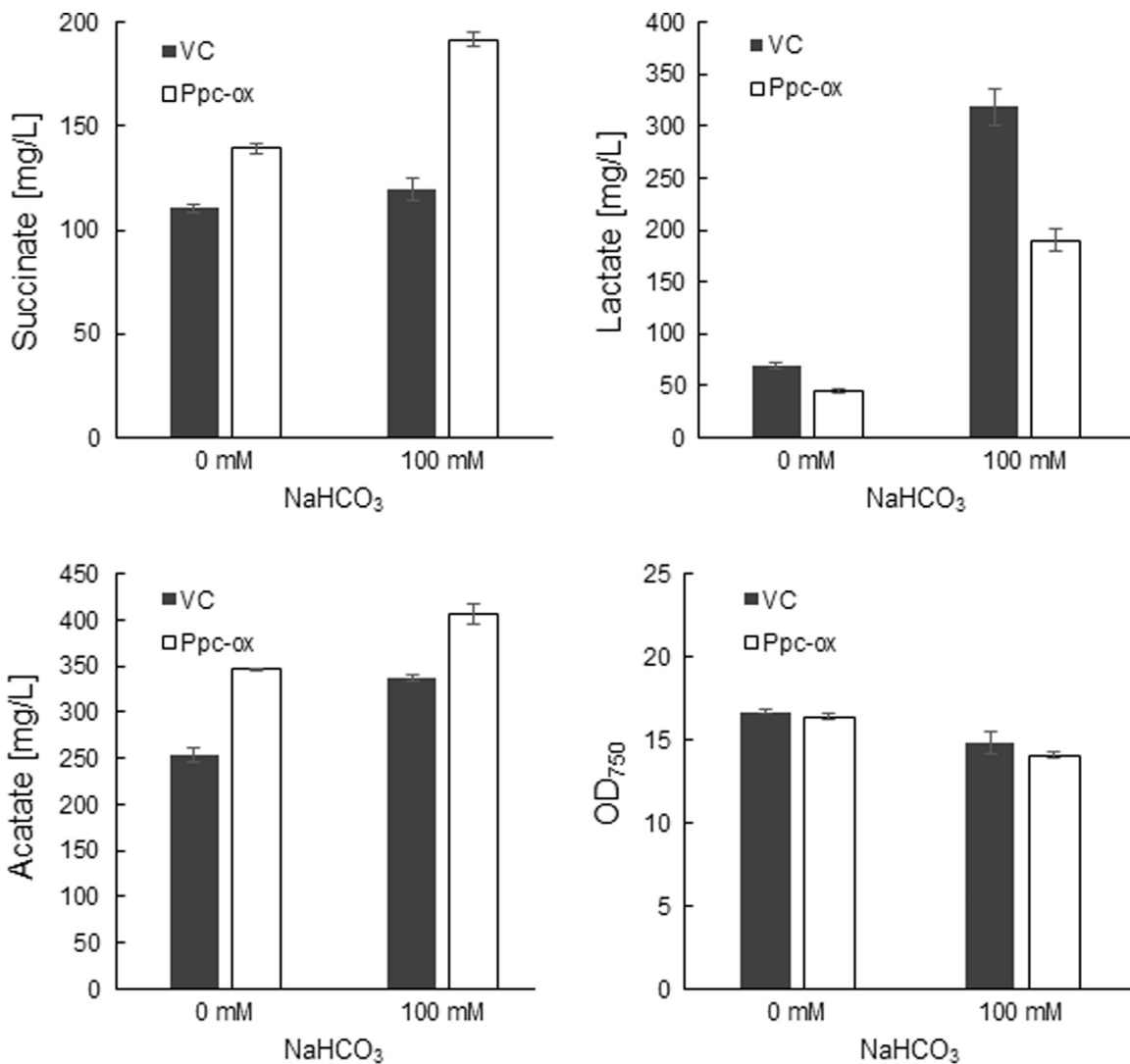
Fig. 5. Organic acid production in Ppc-ox and its vector control strain in the absence or presence of 100 mM NaHCO$_3$. Organic acids and OD$_{750}$ were measured after 72 h fermentation. Values represent the average ($\pm$ SD) of three independent experiments.

improved from 120 mg L^{-1} to 192 mg L^{-1} by *ppc* overexpression (Fig. 5). The addition of ^{13}C-bicarbonate (NaH^{13}CO$_3$) to the medium resulted in the incorporation of ^{13}C in organic acids such as malate, fumarate and succinate (Fig. 7), demonstrating that bicarbonate is a carbon source for succinate production. Citrate and *iso*-citrate were labeled with ^{13}C, and the ^{13}C fraction of 2-ketoglutarate was 9.9% after 24 h. Alanine and lactate, which can be produced from pyruvate, were slightly labeled with ^{13}C. In contrast, PEP, acetyl-CoA, and metabolites involved in glycolysis such as F6P and 3PGA were not enriched in ^{13}C.

4. Discussion

Time-course analyses of the metabolome, transcriptome and metabolic turnover revealed dynamic changes in the metabolism of the cyanobacterium *Synechocystis* sp. PCC6803 cultivated under dark anoxic conditions, allowing identification of the rate-limiting steps in sugar catabolism. In addition, rational metabolic engineering based on these metabolic analyses leads to improved succinate production.

ATP is generated for cell maintenance during auto-fermentative metabolism of glycogen (Kumaraswamy et al., 2013; McNeely et al., 2010), but catabolism has never been observed. In the present study, dynamic metabolic profiling clearly indicated that succinate is biosynthesized by sugar catabolism via glycolysis, the pentose phosphate pathway, the anapletotic pathway, and the reductive TCA cycle, since the ^{12}C atoms in sugar (hexose, pentose and triose) phosphates, organic acids and amino acids were replaced by ^{13}C derived from ^{13}C-glucose during anoxic cultivation (Fig. 4). Succinic acid can be produced via three routes in prokaryotic cells: the reductive and oxidative pathways of the TCA cycle, and the glyoxylate shunt (Choi et al., 2015). However, the cyanobacterial TCA cycle is branched into oxidative and reductive routes (Knoop et al., 2013). The genes involved in the glyoxylate shunt of *Synechocystis* 6803 have not been isolated (Knoop et al., 2013). Recent studies found that the cyanobacterial TCA cycle can be completed via the γ-aminobutyric acid (GABA) shunt constituting a pathway from 2-ketoglutarate, via glutamate, GABA and succinate semialdehyde, to succinate (Xiong et al., 2014) or via 2-ketoglutarate decarboxylase and succinic semialdehyde dehydrogenase (Zhang et al., 2011). However, as shown in Fig. 4, 53% of the ^{12}C was replaced with ^{13}C in succinic acid but only 22% was replaced in 2-ketoglutarate, indicating that succinic acid was produced via the reductive TCA cycle under dark anoxic conditions.

Synechocystis 6803 biosynthesizes glycogen from CO$_2$ assimilated during periods of light exposure (Smith, 1983) and can be
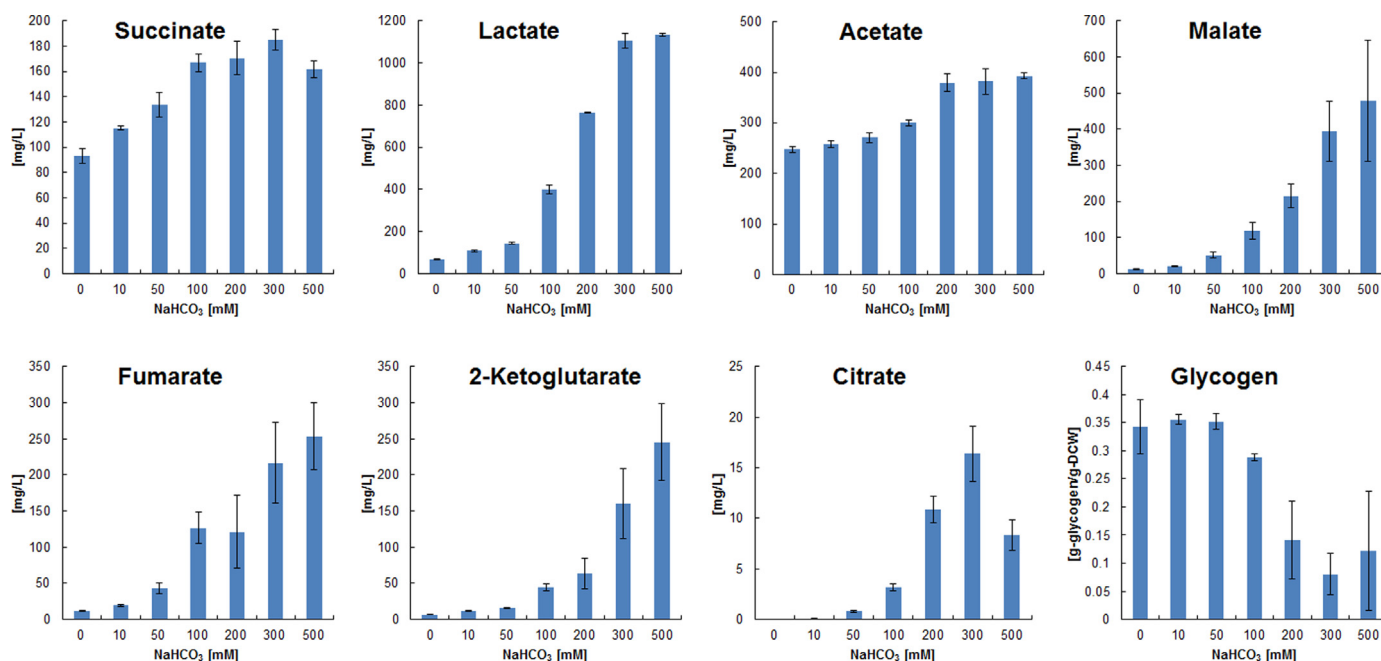
Fig. 6. Effect of NaHCO₃ addition on organic acid production by *Synechocystis* sp. PCC6803 GT strain and its effect on glycogen utilization. Organic acids and glycogen were measured after 72 h fermentation. Values represent the average (± SD) of three independent experiments.

hydrolyzed to glucose 1-phosphate by GP encoded by *glgP* with support from isoamylase encoded by *glgX*, (Ball and Morell, 2003; Fu and Xu, 2006). In the present study, GP activity was higher under dark anoxic conditions than under light conditions (Fig. 2). Our metabolic analyses elucidated the biological route for succinic acid production from glycogen under dark anoxic conditions, as illustrated in Fig. 3.

Carbon distribution and redox balance during autofermentation have been estimated (McNeely et al., 2010, 2014) but the *in vivo* kinetics of these processes have not previously been investigated. Direct measurement of metabolic turnover using the described *in vivo* ^{13}C-labeling assay demonstrated that there is a rate-limiting step between PEP and oxaloacetate under dark anoxic conditions and that overexpression of PEP carboxylase and the addition of bicarbonate improved succinate production (Fig. 5). *In vivo* labeling with ^{13}C-bicarbonate clearly showed carbon incorporation into succinate via the anaplerotic pathway and the reductive TCA cycle (Fig. 7). However, the initial slope of succinate was lower than that of fumarate, indicating that the conversion of fumarate to succinate is also a rate-limiting step in succinate biosynthesis. ^{13}C fraction of succinate was lower than 20% after 24 h fermentation, which should be due to glycogen catabolism.

Time-course metabolome analysis indicated other potential rate-limiting steps in succinic acid production. As shown in Fig. 3, G1P increased with time in cells grown with NH₄Cl and reached 11.9 μmol g-DCW^{-1} after 96 h of fermentation, whereas the level of G6P formed from G1P by phosphoglucomutase remained essentially constant (0.3–0.6 μmol g-DCW^{-1}). This raises the possibility that phosphoglucomutase is a rate-limiting step in glycogen catabolism. The FBP level increased from 0.05 to 6.18 μmol g-DCW^{-1} after 3 h of fermentation and then remained constant, while there were only trace levels of DHAP and GAP, suggesting that FBP aldolase is a rate-limiting step in sugar catabolism. Glycogen catabolism might be improved by increasing the concentrations of phosphoglucomutase and FBP aldolase. Interestingly, ATP levels increased from 0 h to 24 h, then decreased. The catabolism of glycogen can generate ATP during autofermentation. ATP might be used by ATP-citrate lyase (ACL), which converts citrate to acetyl-CoA and oxaloacetate in the reductive TCA cycle

(Fig. 3), although genes encoding ALC have not been isolated from *Synechocystis* 6803.

As shown in Fig. 1, no secretion of succinate was detected from 0 h to 6 h, possibly due to slow ^{13}C incorporation into intracellular succinate between 0 and 2 h (Fig. 4). Intracellular pool size analysis (Fig. 3) showed that maximum levels of acetyl-CoA, citrate, *cis*-aconitate and *iso*-citrate were obtained after 6 h, while malate, fumarate and succinate increased until 24 h. The expression of *acnB* was downregulated after 3 h of fermentation (Table 2). These data suggest that the major carbon flow in the TCA cycle changes from the oxidative to the reductive route during fermentation.

Global gene expression analysis showed that genes involved in light harvesting, photosystems, photosynthetic electron transport and Rubisco were downregulated under dark anoxic conditions (Table 2), likely due to the switching of cyanobacterial metabolism from photoautotrophism to carbohydrate catabolism. The expression of *nifJ* encoding PFO (Schmitz et al., 2001) increased under anoxic conditions. PFO catalyzes the oxidative cleavage of pyruvate and coenzyme A to acetyl-CoA and CO₂, with the simultaneous reduction of ferredoxin or flavodoxin. Under dark anoxic conditions, the expression of *nifJ* might be enhanced to supply reductants such as reduced ferredoxin and flavodoxin, and NADH for organic acid production. It was previously shown that overexpression of NAD$^+$-dependent GAP dehydrogenase in *Synechococcus* sp. PCC7002 increased glycogen catabolic capacity, with a concomitant increase in terminal fermentation products, likely due to an increased NADH/NAD$^+$ ratio (Kumaraswamy et al., 2013). The removal of nitrate from the culture medium enhances auto-fermentative hydrogen production in *Synechococcus* sp. PCC7002 (McNeely et al., 2014). Since nitrate is reduced to NH₄$^+$ by nitrate reductase, reductants required for nitrate assimilation are consumed following nitrate removal. In the present study, *Synechocystis* 6803 cultivated in the presence of NH₄Cl showed higher organic acid production than when cultivated in the presence of NaNO₃ (Fig. 1), perhaps due to the high accumulation of reductants in cells phototrophically cultivated in the presence of NH₄Cl.

Carbon capture and utilization has recently attracted increasing attention as a route to developing an environmentally benign
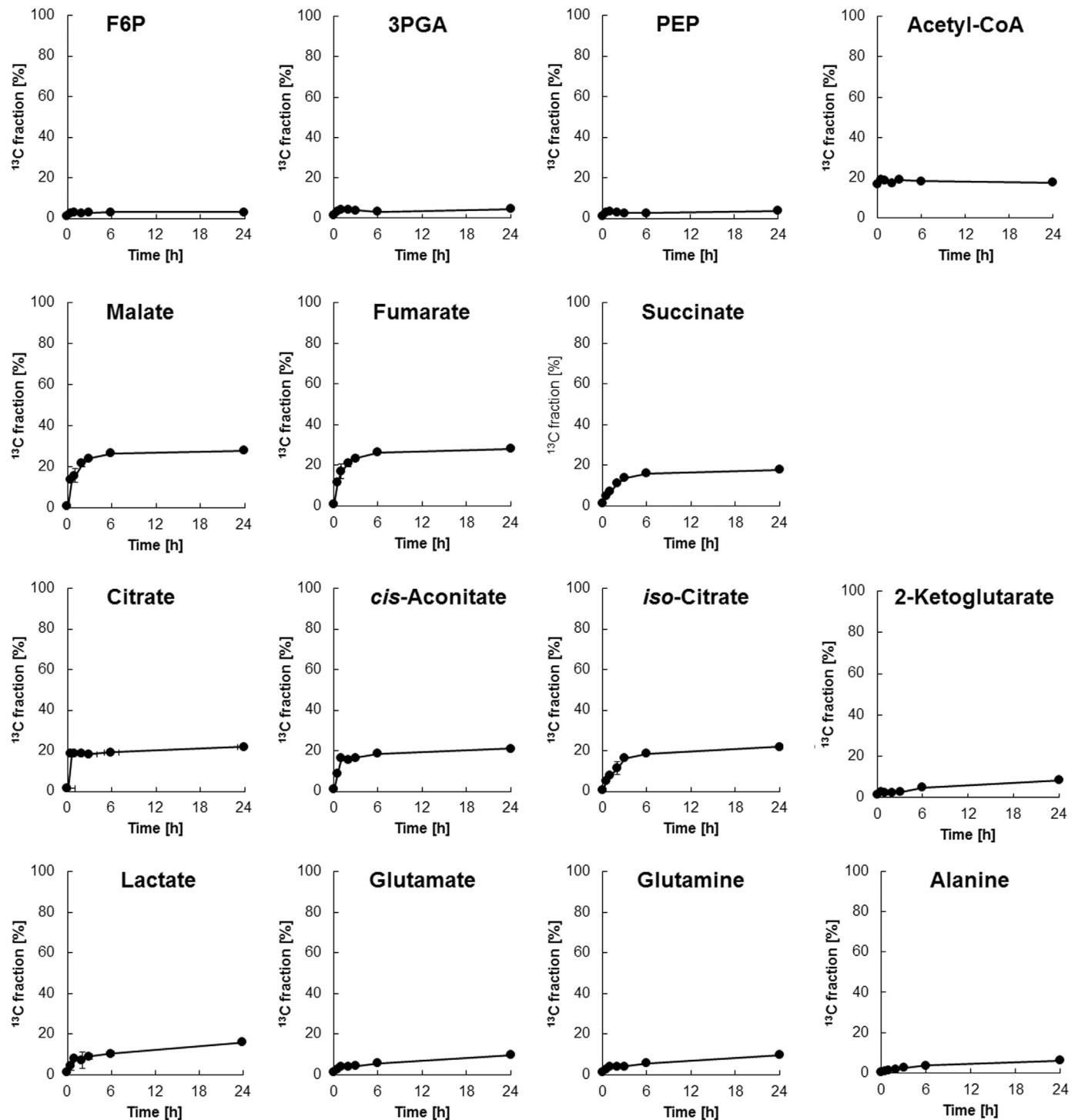
Fig. 7. Time-course changes in the metabolite ^{13}C fraction following the addition of ^{13}C-bicarbonate. Each data point represents the average ($\pm$ SD) of three independent experiments.

society (von der Assen et al., 2014). The amount of succinate produced by cyanobacteria is lower than that of several strains of rumen bacteria, fungi and metabolically-engineered microorganisms, but they require no carbon source other than CO_2. Increased levels of organic acids were observed following the addition of HCO_3^-, which is in equilibrium with CO_2 ($pK_a = 6.35$) (Fig. 5), suggesting that the addition of CO_2 to the culture can improve succinic acid production via the anaplerotic pathway. Phototrophic cyanobacteria therefore hold great promise for the effective utilization of CO_2.

Acknowledgements

Appendix A. Supplementary material

Supplementary data associated with this article can be found in the online version at http://dx.doi.org/10.1016/j.meteno.2016.04.003.

References

Aikawa, S., Joseph, A., Yamada, R., Izumi, Y., Yamagishi, T., Matsuda, F., Kawai, H., Chang, J.S., Hasunuma, T., Kondo, A., 2013. Direct conversion of *Spirulina* to ethanol without pretreatment or enzymatic hydrolysis process. Energy Environ. Sci. 6, 1844–1849. http://dx.doi.org/10.1039/C3EE40305J.

Anfelt, J., Kaczmarzyk, D., Shabestary, K., Renberg, B., Rockberg, J., Nielsen, J., Uhlén, M., Hudson, E.P., 2015. Genetic and nutrient modulation of acetyl-CoA levels in *Synechocystis* for *n*-butanol production. Microb. Cell Fact. 14, 167.

Aikawa, S., Nishida, A., Ho, S.-H., Chang, J.S., Hasunuma, T., Kondo, A., 2014. Glycogen production for biofuels by the euryhaline cyanobacteria *Synechococcus* sp strain PCC 7002 from an oceanic environment. Biotechnol. Biofuels 7, 88. http://dx.doi.org/10.1186/1754-6834-7-88.

Akhtar, J., Idris, A., Abd Aziz, R., 2014. Recent advances in production of succinic acid from lignocellulosic biomass. Appl. Microbiol. Biotechnol. 98, 987–1000. http://dx.doi.org/10.1007/s00253-013-5319-6.

Andersen, B., Westergaard, N., 2002. The effect of glucose on the potency of two distinct glycogen phosphorylase inhibitors. Biochem. J. 367, 443–450. http://dx.doi.org/10.1042/BJ20020153.

Ball, S.G., Morell, M.K., 2003. From bacterial glycogen to starch: understanding the biogenesis of the plant starch granule. Annu. Rev. Plant Biol. 54, 207–233. http://dx.doi.org/10.1146/annurev.arplant.54.031902.134927.

Beauprez, J.J., De Mey, M., Soetaert, W.K., 2010. Microbial succinic acid production: natural *versus* metabolic engineered producers. Process Biochem. 45, 1103–1114. http://dx.doi.org/10.1016/j.procbio.2010.03.035.

Bozell, J.J., Peterson, G.R., 2010. Technology development for the production of biobased products from biorefinery carbohydrates – the US Department of Energy's "Top 10" revisited. Green Chem. 12, 539–554. http://dx.doi.org/10.1039/B922014C.

Camañes, G., Scalschi, L., Vicedo, B., González-Bosch, C., García-Agustín, P., 2015. An untargeted global metabolomic analysis reveals the biochemical changes underlying basal resistance and priming in *Solanum lycopersicum* and identifies 1-methyltryptophan as a metabolite involved in plant responses to *Botrytis cinerea* and *Pseudomonas syringae*. Plant J. 84, 125–139. http://dx.doi.org/10.1111/tpj.12964.

Chen, L.M., Omiya, T., Hata, S., Izui, K., 2002. Molecular characterization of a phosphoenolpyruvate carboxylase from a thermophilic cyanobacterium, *Synechococcus vulcanus* with unusual allosteric properties. Plant Cell Physiol. 43, 159–169. http://dx.doi.org/10.1093/pcp/pcf019.

Chen, Y., Nielsen, J., 2013. Advances in metabolic pathway and strain engineering paving the way for sustainable production of chemical building blocks. Curr. Opin. Biotechnol. 24, 965–972. http://dx.doi.org/10.1016/j.copbio.2013.03.008.

Choi, S., Song, C.W., Shin, J.H., Lee, S.Y., 2015. Biorefineries for the production of top building block chemicals and their derivatives. Metab. Eng. 28, 223–239. http://dx.doi.org/10.1016/j.ymben.2014.12.007.

Cukalovic, A., Stevens, C.V., 2008. Feasibility of production methods for succinic acid derivatives: a marriage of renewable resources and chemical technology. Biofuels Bioprod. Bioref. 2, 505–529. http://dx.doi.org/10.1002/bbb.105.

Delhomme, C., Weuster-Botz, D., Kühn, F.E., 2009. Succinic acid from renewable resources as a C_4 building-block chemical – a review of the catalytic possibilities in aqueous media. Green. Chem. 11, 13–26. http://dx.doi.org/10.1039/B810684C.

Diamond, S., Jun, D., Rubin, B.E., Golden, S.S., 2015. The circadian oscillator in *Synechococcus elongatus* controls metabolite partitioning during diurnal growth. Proc. Natl. Acad. Sci. USA 112, E1916–E1925. http://dx.doi.org/10.1073/pnas.1504576112.

Dismukes, G.C., Carrieri, D., Bennette, N., Ananyev, G.M., Posewitz, M.C., 2008. Aquatic phototrophs: efficient alternatives to land-based crops for biofuels. Curr. Opin. Biotechnol. 19, 235–240. http://dx.doi.org/10.1016/j.copbio.2008.05.007.

Fu, J., Xu, X., 2006. The functional divergence of two *glgP* homologues in *Synechocystis* sp. PCC6803. FEMS Microbiol. Lett. 260, 201–209. http://dx.doi.org/10.1111/j.1574-6968.2006.00312.x.

Hasunuma, T., Harada, K., Miyazawa, S., Kondo, A., Fukusaki, E., Miyake, C., 2010. Metabolic turnover analysis by a combination of *in vivo* ^{13}C-Labeling from ^{13}CO$_2$ and metabolic profiling with CE-MS/MS reveals rate-limiting steps of the C_3 photosynthetic pathway in *Nicotiana tabacum* leaves. J. Exp. Bot. 61, 1041–1051. http://dx.doi.org/10.1093/jxb/erp374.

Hasunuma, T., Kikuyama, F., Matsuda, M., Aikawa, S., Izumi, Y., Kondo, A., 2013. Dynamic metabolic profiling of cyanobacterial glycogen biosynthesis under conditions of nitrate depletion. J. Exp. Bot. 64, 2943–2954. http://dx.doi.org/10.1093/jxb/ert134.

Hasunuma, T., Matsuda, M., Senga, Y., Aikawa, S., Toyoshima, M., Shimakawa, G., Miyake, C., Kondo, A., 2014. Overexpression of *flv3* improves photosynthesis in the cyanobacterium *Synechocystis* sp. PCC6803 by enhancement of alternative electron flow. Biotechnol. Biofuels 7, 493. http://dx.doi.org/10.1186/s13068-014-0183-x.

Izumi, Y., Aikawa, S., Matsuda, F., Hasunuma, T., Kondo, A., 2013. Aqueous sizeexclusion chromatographic method for the quantification of cyanobacterial native glycogen. J. Chromatogr. B Anal. Technol. Biomed. Life Sci. 930, 90–97. http://dx.doi.org/10.1016/j.jchromb.2013.04.037.

Kaneko, T., Sato, S., Kotani, H., Tanaka, A., Asamizu, E., Nakamura, Y., Miyajima, N., Hirosawa, M., Sugiura, M., Sasamoto, S., Kimura, T., Hosouchi, T., Matsuno, A.,

Muraki, A., Nakazaki, N., Naruo, K., Okumura, S., Shimpo, S., Takeuchi, C., Wada, T., Watanabe, A., Yamada, M., Yasuda, M., Tabata, S., 1996. Sequence analysis of the genome of the unicellular cyanobacterium *Synechocystis* sp. strain PCC6803. II. Sequence determination of the entire genome and assignment of potential protein-coding region. DNA Res. 3, 109–136. http://dx.doi.org/10.1093/dnares/3.3.109.

Knoop, H., Gründel, M., Zilliges, Y., Lehmann, R., Hoffmann, S., Lockau, W., Steuer, R., 2013. Flux balance analysis of cyanobacterial metabolism: the metabolic network of *Synechocystis* sp. PCC 6893. PLoS Comput. Biol. 9, e1003081. http://dx.doi.org/10.1371/journal.pcbi.1003081.

Kumaraswamy, G.K., Guerra, T., Qian, X., Zhang, S., Bryant, D.A., Dismukes, G.C., 2013. Reprogramming the glycolytic pathway for increased hydrogen production in cyanobacteria: metabolic engineering of NAD$^+$ -dependent GAPDH. Energy Environ. Sci. 6, 3722–3731. http://dx.doi.org/10.1039/C3EE42206B.

Lee, J., Sim, S.J., Bott, M., Um, Y., Oh, M.K., Woo, H.M., 2014. Succinate production from CO$_2$-grown microalgal biomass as carbon source using engineered *Corynebacterium glutamicum* through consolidated bioprocessing. Sci. Rep. 4, 5819. http://dx.doi.org/10.1038/srep05819.

Link, H., Kochanowski, K., Sauer, U., 2013. Systematic identification of allosteric protein-metabolite interactions that control enzyme activity *in vivo*. Nat. Biotechnol. 31, 357–361. http://dx.doi.org/10.1038/nbt.2489.

McNeely, K., Xu, Y., Bennette, N., Bryant, D.A., Dismukes, G.C., 2010. Redirecting reductant flux into hydrogen production via metabolic engineering of fermentative carbon metabolism in a cyanobacterium. Appl. Environ. Microbiol. 76, 5032–5038. http://dx.doi.org/10.1128/AEM.00862-10.

McNeely, K., Kumaraswamy, G.K., Guerra, T., Bennette, N., Ananyev, G., Dismukes, G. C., 2014. Metabolic switching of central carbon metabolism in response to nitrate: application to autofermentative hydrogen production in cyanobacteria. J. Biotechnol. 182–183, 83–91. http://dx.doi.org/10.1016/j.jbiotec.2014.04.004.

Osanai, T., Oikawa, A., Azuma, M., Tanaka, K., Saito, K., Hirai, M.Y., Ikeuchi, M., 2011. Genetic engineering of group 2 σ factor SigE widely activates expression of sugar catabolic genes in *Synechocystis* species PCC 6803. J. Biol. Chem. 286, 30962–30971. http://dx.doi.org/10.1074/jbc.M111.231183.

Osanai, T., Shirai, T., Iijima, H., Nakaya, Y., Okamoto, M., Kondo, A., Hirai, M.Y., 2015. Genetic manipulation of a metabolic enzyme and a transcriptional regulator increasing succinate excretion from unicellular cyanobacterium. Front. Microbiol. 6, 1064. http://dx.doi.org/10.3389/fmicb.2015.01064.

Partensky, F., Hess, W.R., Vaulot, D., 1999. *Prochlorococcus*, a marine photosynthetic prokaryote of global significance. Microbiol. Mol. Biol. Rev. 63, 106–127.

Rippka, R., Deruelles, J., Waterbury, J.B., Herdman, M., Stanier, R.Y., 1979. Generic assignments, strains histories and properties of pure culture of cyanobacteria. J. Gen. Microbiol. 111, 1–61. http://dx.doi.org/10.1099/00221287-111-1-1.

Savakis, P.E., Angermayr, S.A., Hellingwerf, K.J., 2013. Synthesis of 2,3-butanediol by *Synechocystis* sp. PCC6803 via heterologous expression of a catabolic pathway from lactic acid- and enterobacteria. Metab. Eng. 20, 121–130. http://dx.doi.org/10.1016/j.ymben.2013.09.008.

Schmitz, O., Gurke, J., Bothe, H., 2001. Molecular evidence for the aerobic expression of *nifJ*, encoding pyruvate:ferredoxin oxidoreductase, in cyanobacteria. FEMS Microbiol. Lett. 195, 97–102. http://dx.doi.org/10.1016/S0378-1097(00)00558-9.

Smith, A.J., 1983. Modes of cyanobacterial carbon metabolism. Ann. Microbiol. 134B, 93–113. http://dx.doi.org/10.1016/S0769-2609(83)80099-4.

Tsuge, Y., Tateno, T., Sasaki, K., Hasunuma, T., Tanaka, T., Kondo, A., 2013. Direct production of organic acids from starch by cell surface-engineered *Corynebacterium glutamicum* in anaerobic conditions. AMB Express 3, 72. http://dx.doi.org/10.1186/2191-0855-3-72.

Varman, A.M., Xiao, Y., Pakrasi, H.B., Tang, Y.J., 2013. Metabolic engineering of *Synechocystis* sp. strain PCC 6803 for isobutanol production. Appl. Environ. Microbiol. 79, 908–914. http://dx.doi.org/10.1128/AEM.02827-12.

von der Assen, N., Voll, P., Peters, M., Bardow, A., 2014. Life cycle assessment of CO$_2$ capture and utilization: a tutorial review. Chem. Soc. Rev. 43, 7982–7994. http://dx.doi.org/10.1039/c3cs60373c.

Wang, Y., Sun, T., Gao, X., Shi, M., Wu, L., Chen, L., Zhang, W., 2016. Biosynthesis of platform chemical 3-hydroxypropionic acid (3-HP) directly from CO$_2$ in cyanobacterium *Synechocystis* sp. PCC 6803. Metab. Eng. 34, 60–70. http://dx.doi.org/10.1016/j.ymben.2015.10.008.

Wijffels, R.H., Kruse, O., Hellingwerf, K.J., 2013. Potential of industrial biotechnology with cyanobacteria and eukaryotic microalgae. Curr. Opin. Biotechnol. 24, 405–413.

Williams, J.G.K., 1988. Construction of specific mutations in photosystem II photosynthetic reaction center by genetic engineering methods in *Synechocystis* 6803. Methods Enzymol. 167, 766–778. http://dx.doi.org/10.1016/0076-6879(88)67088-1.

Xiong, W., Brune, D., Vermaas, W.F.J., 2014. The γ-aminobutyric acid shunt contributes to closing the tricarboxylic acid cycle in *Synechocystis* sp. PCC 6803. Mol. Microbiol. 93, 786–796. http://dx.doi.org/10.1111/mmi.12699.

Zhang, S., Bryant, D.A., 2011. The tricarboxylic acid cycle in cyanobacteria. Science 334, 1551–1553. http://dx.doi.org/10.1126/science.1210858.

Zhou, J., Zhang, H., Zhang, Y., Li, Y., Ma, Y., 2012. Designing and creating a modularized synthetic pathway in cyanobacterium *Synechocystis* enables production of acetone from carbon dioxide. Metab. Eng. 14, 394–400. http://dx.doi.org/10.1016/j.ymben.2012.03.005.